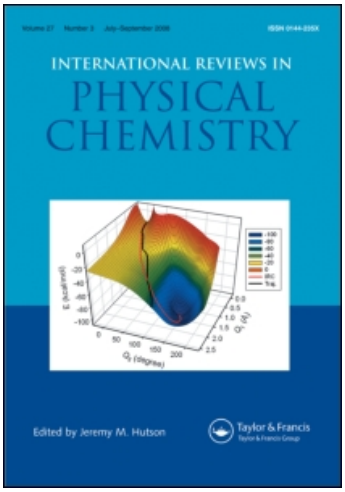

International Reviews in Physical Chemistry
Publication details, including instructions for authors and subscription information:
http://www.informaworld.com/smpp/title~content=t713724383

Chemical reactions in quantum crystals

Takamasa Momose[a]; Mizuho Fushitani[b]; Hiromichi Hoshina[b]
[a] Department of Chemistry, The University of British Columbia, Vancouver, British Columbia V6T1Z1, Canada [b] Department of Chemistry, Graduate School of Science, Kyoto University, Kyoto 606-8502, Japan

To cite this Article Momose, Takamasa , Fushitani, Mizuho and Hoshina, Hiromichi(2005) 'Chemical reactions in quantum crystals', International Reviews in Physical Chemistry, 24: 3, 533 — 552
To link to this Article: DOI: 10.1080/01442350500444107
URL: http://dx.doi.org/10.1080/01442350500444107

International Reviews in Physical Chemistry,
Vol. 24, Nos. 3–4, July–December 2005, 533–552

Taylor & Francis
Taylor & Francis Group

Chemical reactions in quantum crystals

TAKAMASA MOMOSE*†, MIZUHO FUSHITANI‡§ and
HIROMICHI HOSHINA‡¶

†Department of Chemistry, The University of British Columbia,
2036 Main Mall, Vancouver, British Columbia V6T1Z1, Canada
‡Department of Chemistry, Graduate School of Science,
Kyoto University, Kyoto 606-8502, Japan

(*Received 21 July 2005; in final form 10 October 2005*)

Solid parahydrogen, known as a quantum crystal, is a novel matrix for the study of physical and chemical processes of molecules at low temperatures by high-resolution infrared spectroscopy. Ro-vibrational motion of molecules embedded in solid parahydrogen is well quantized on account of the weak interaction in the crystal. In addition, molecules are almost free from the cage effect because of the softness of the quantum crystal, so that a variety of chemical reactions could be observed for molecules in solid parahydrogen at liquid He temperatures. In this article, we survey our recent studies on photodissociation of methyl radicals and subsequent reactions in solid parahydrogen, and discuss (1) the nuclear spin selection rule in chemical reactions and (2) pure tunnelling reactions obtained from the analysis of the present system.

Contents

*Corresponding author. Email: momose@chem.ubc.ca
§Present address: Institute fur Experimentalphysik, Fachbereich Physik, Freie Universitat Berlin, Germany.
¶Present address: Kawase Initiative Research Unit, RIKEN, Wako, Japan.

International Reviews in Physical Chemistry
ISSN 0144–235X print/ISSN 1366–591X online © 2005 Taylor & Francis
http://www.tandf.co.uk/journals
DOI: 10.1080/01442350500444107

1. Introduction

Matrix isolation spectroscopy, initially introduced by Lewis *et al.* [1], has been used for a variety of applications in the field of physical chemistry [2, 3]. Matrices of rare gas atoms such as Ne and Ar have been widely used because of their chemically inert property and weak perturbations. Needless to say, its application to unstable molecules has piloted studies on spectroscopy and chemical dynamics in the gas phase [2]. The resolution is, however, inherently limited due to both homogeneous and inhomogeneous line broadening, and the broadness of spectra hides some information that might provide detailed information on interactions and dynamics of molecules in condensed phases. In addition, the rigidity of these conventional matrices limits the study of chemical reactions at cryogenic temperatures, as strong interactions from the surrounding lattice may distort reaction potential surfaces significantly from those in the gas phase [4–8].

Recently, we have conducted spectroscopy of molecules embedded in solid parahydrogen crystals, and found unique properties of solid parahydrogen as a host for matrix isolation spectroscopy [9–12]. First of all, not only the vibrational energy levels, but also the rotational energy levels of molecules are well-quantized in solid parahydrogen [12–15]. Secondly, the lifetime of these quantized rotation–vibration excited states is extremely long, so that high-resolution spectroscopy can be applied to molecules in solid parahydrogen as in the gas phase [12, 16, 17]. The spectral linewidth is sharp enough to resolve not only their rotational structures, but also fine spectral structures originating in subtle interactions in the crystal, and the analysis of such fine structures gives us rich information on intermolecular interactions as well as the motion of the molecule in the condensed phase. Thirdly, molecules are almost free from the cage effect because of the softness of the quantum crystal, so that a variety of chemical reactions could be observed for molecules in solid parahydrogen at liquid He temperatures [9, 11, 18–23]. Availing these unique properties, matrix isolation spectroscopy in solid parahydrogen has been applied to the study of physical and chemical processes of molecules in this novel quantum crystal by several groups [11, 12, 24–35].

In this article, we focus on chemical reactions that take place in solid parahydrogen crystals. Matrix isolation spectroscopy in solid parahydrogen has many advantages over other techniques in studying chemical reaction dynamics at low temperatures. Molecules in solid parahydrogen at liquid He temperatures occupy only a limited number of its rotational levels, mostly the $J=0$ ground rotational level only. Therefore, reactions in solid parahydrogen themselves can be considered as state selective reactions, which give us quantitative information on the state dependent phenomena for a variety of reactions. As an example, examination of the nuclear spin selection rule in chemical reactions will be discussed in section 5 [36].

Another important phenomenon in solid parahydrogen is the occurrence of tunnelling chemical reactions [18, 23]. Tunnelling effects become dominant at low temperatures in most reactions, but few studies have been reported due to the difficulty in making reaction systems at low temperatures. We found that some radicals produced in solid parahydrogen induce tunnelling reaction with a nearby hydrogen molecule. Details will be discussed in section 6.

The reaction system we discuss in this article is the photolysis of methyl iodide embedded in solid parahydrogen, and its subsequent reactions. The reaction system has been studied extensively in the gas phase. Despite the simplicity, the present system gave us rich information which is fundamental to physical and chemical processes of molecules at low temperatures.

This article is organized as follows. First, we briefly overview properties of the parahydrogen matrix in section 2. Experimental setups are given in section 3. Then, details of the reactions subsequently induced by the photolysis of methyl iodides are described in section 4. Two important results obtained from the analysis of the present reaction system, that is, the nuclear spin selection rule in the chemical reactions, and the observation of pure tunnelling reactions, are discussed in sections 5 and 6, respectively.

2. Solid parahydrogen as a matrix

The rotational angular momentum J of each hydrogen molecule is well defined, remaining a good quantum number in solid hydrogen because of the weak interaction between hydrogen molecules [37]. The Pauli exclusion principle requires that the rotational states having even quantum numbers must couple with the $I=0$ nuclear spin state, while those having odd quantum numbers couple with the $I=1$ nuclear spin state, exclusively. The former is called parahydrogen, and the latter orthohydrogen. At very low temperatures, parahydrogen occupies only the $J=0$ rotational level, while orthohydrogen occupies the $J=1$ level. Relaxation from the $J=1$ rotational state to the $J=0$ state is extremely slow even in solid hydrogen [37], and parahydrogen and orthohydrogen can be treated as almost different molecules in solid parahydrogen.

Since the $J=0$ rotational wavefunction has a spherical shape, parahydrogen molecules at liquid He temperatures have no permanent electric moments of any order. On the other hand, orthohydrogen molecules occupying the $J=1$ rotational quantum number have a small permanent quadrupole moment. The quadrupole moment of the $J=1$ orthohydrogen provides slightly stronger interaction with its surroundings than the $J=0$ parahydrogen. Therefore, the concentration of orthohydrogen in parahydrogen matrices needs to be as low as possible in order that molecules in solid parahydrogen may be least perturbed. Since the $J=1$ orthohydrogen has about $120\,\mathrm{cm}^{-1}$ higher energy than the $J=0$ parahydrogen, the concentration of orthohydrogen can be reduced to less than 0.05% by using an ortho–para converter [11, 25] operated at just above the melting point of 13.8K. The concentration of orthohydrogen in our sample described in this article was always less than 0.1%.

One of the prominent features of the quantum crystal is the large amplitude of zero-point lattice vibration [38]. The mean amplitude of the zero-point vibration in solid parahydrogen amounts to almost 20% of the intermolecular distance [39]. As a result, the intermolecular distance in solid parahydrogen (3.78 Å) is considerably larger than the interatomic distance in solid Ne (3.16 Å), although the pair potential between H_2 molecules is similar to the potential between Ne atoms [12]. The large lattice constant and the large amplitude of zero-point lattice vibration in solid hydrogen provides more free space for guest molecules than other matrices. Moreover, because

of the large lattice constant of solid parahydrogen, interactions between the guest molecule and surrounding host molecules become weak compared with those in Ne matrix. As a result, the lifetime of excited states of a guest molecule in solid parahydrogen becomes much longer, which must be the origin of the sharp spectral linewidth in solid parahydrogen.

Another important feature of solid parahydrogen is its high thermal conductivity. At liquid He temperatures, the thermal conductivity of solid parahydrogen containing 0.2% orthohydrogen is $50\,W\,m^{-1}\,K^{-1}$ [39], which is comparable to that of Cu, and is almost one order of magnitude larger than the conductivity of rare gas crystals [40]. The high thermal conductivity of solid parahydrogen must play an important role in the photodissociation processes, as it will lead to the fast dissipation of excess energy produced by photolysis and as a result the photofragments may be stably isolated in the crystal quickly.

3. Experiments

Since H_2 has relatively high vapour pressure even at liquid He temperatures [41], the standard deposition technique which is usually employed for isolation spectroscopy of rare gas matrices does not work straightforwardly. Three different techniques have been developed so far to make transparent parahydrogen matrices [11, 25, 34]. Fajardo *et al.* have found a condition for growing completely transparent crystals of millimetre thickness by controlling the deposition rate and the temperature of the substrate [24, 25]. Recently, Lee *et al.* developed another deposition technique based on the supersonic expansion of mixed gas onto the cold surface [34]. Our method of crystal growth is different from those developed by Fajardo *et al.* and Lee *et al.* We grew our crystals in an enclosed cell [11], which was initially used by Oka *et al.* in their high-resolution spectroscopy of solid parahydrogen itself [16].

The enclosed cell is a cylindrical copper cell with both ends closed off by BaF_2 windows with indium gaskets. The pure parahydrogen gas containing orthohydrogen of less than 0.05% was obtained by passing high purity (>99.9995%) normal hydrogen gas through an ortho–para converter operated at 14 K. Details of the converter are described in a previous review article [11]. About 10 PPM of dopant gas was mixed with the converted hydrogen gas at room temperature. Subsequently, the mixed gas was continuously introduced through a thin stainless inlet tube into the copper cell installed under the cold surface of a standard liquid He optical cryostat. A small percentage of the dopant molecule escapes condensation in the inlet tube and becomes incorporated into the parahydrogen solid. The temperature of the sample cell was kept at around 7–8K during the growth of the crystal. The sample was then cooled to ~4K for observation. All the measurements in this article were done at around 4.5K. The crystal grown in this manner was completely transparent.

For the photolysis of methyl iodide, we used a low-pressure 20 W mercury lamp, which emits UV light at 253.7 nm and 184.9 nm. To effect the selective photolysis at 253.7 nm, a Toshiba UV-25 cutoff filter was used. Since the filter transmits wavelengths longer than 200 nm, light at 184.9 nm can be completely cut while light at

253.7 nm is transmitted by about 60%. For the photolysis of methyl radicals, we used 193 nm UV pulses from an ArF excimer laser (6 mJ/pulse, 30 Hz).

The infrared absorption spectra were observed by a Fourier transform infrared (FTIR) spectrometer (Bruker IFS-120H) with a resolution of 0.1 cm^{-1} or higher. A globar source, KBr beam splitter and a liquid N_2 cooled HgCdTe (MCT) detector were used for the measurements of absorption spectra in the mid-IR region.

4. Photochemistry of methyl iodide

In the gas phase, methyl iodide is photolysed to a methyl radical and an iodine atom efficiently by UV photons. On the contrary, it has been reported that photolysis of methyl iodide in solid Ne does not yield a methyl radical and an iodine by any light [5–8]. The strong cage effect prevents the photofragments from being separated.

In a series of works, we have shown that alkyl iodide molecules are readily photolysed to alkyl radicals and an iodine atom in solid parahydrogen [9, 19, 36, 42], which is in remarkable contrast to the conventional rigid rare gas matrices. The advantageous feature of the mitigation of the cage effect in solid parahydrogen is attributable to the quantum nature of solid parahydrogen as described in section 2. A large lattice constant and a large amplitude of the zero-point lattice vibration makes solid parahydrogen a spacious and soft lattice for foreign molecules. In addition, a large thermal conductivity of solid parahydrogen [39] may play an important role; the excess energy imparted to nascent photofragments could be quickly removed and the fragments are rapidly frozen to be protected from geminate recombination.

Figure 1 shows the changes of the infrared absorption spectrum of a parahydrogen crystal containing a small amount of CH_3I. Trace (a) is the spectrum as grown and recorded before UV irradiation. Trace (b) is the spectrum recorded after half-day irradiation with 253.7 nm photons. Trace (c) is the spectrum recorded after irradiation with 193 nm UV pulses for 20 min. The irradiation at 193 nm was done just after the half-day irradiation at 253.7 nm.

Absorptions at 2965 cm^{-1} and 3058 cm^{-1} (weak) are assigned to the CH stretching modes of CH_3I. A doublet at 3170 cm^{-1} that appeared after the 253.7 nm irradiation is assigned to the ν_3 mode of CH_3 radical. Multiple peaks in the region of 3000–3050 cm^{-1} that appeared after the 193 nm irradiation are assigned to the ν_3 mode of CH_4.

Figure 2 shows the changes of infrared absorption of a parahydrogen crystal containing CD_3I. The spectra shown in traces (a), (b) and (c) were observed under the same condition as in figure 1. Traces (d) and (e) are the absorption spectra of isolated CD_3H and CD_2H_2 in solid parahydrogen observed separately [12]. Since absorptions corresponding to CD_3I appear outside of the range shown in figure 2, no absorption peaks are seen in trace (a) in figure 2. Multiple peaks in the region of 3390–3410 cm^{-1} after the 253.7 nm irradiation are assigned to the $\nu_3 + \nu_4$ combination band of CD_3 radical. All the multiple peaks in the spectral range of 2960–3030 cm^{-1} in trace (c) are assigned to the transitions of CD_3H (ν_1) and CD_2H_2 (ν_1 and ν_6) as seen in traces (d) and (e).

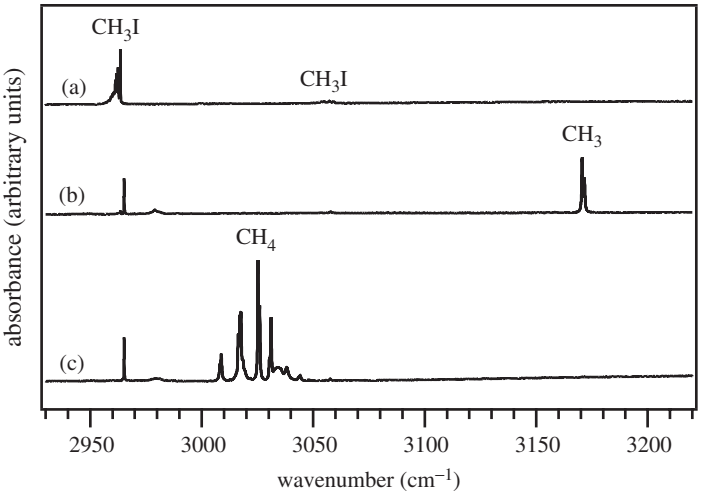

Figure 1. Infrared absorption spectra of CH_3I in solid parahydrogen in the spectral region 2 930–3 220 cm^{-1}. Trace (a): the sample as deposited and recorded before UV irradiation. Trace (b): after half-day irradiation with 253.7 nm photons. Trace (c): after subsequent irradiation with 193 nm photons for 20 min.

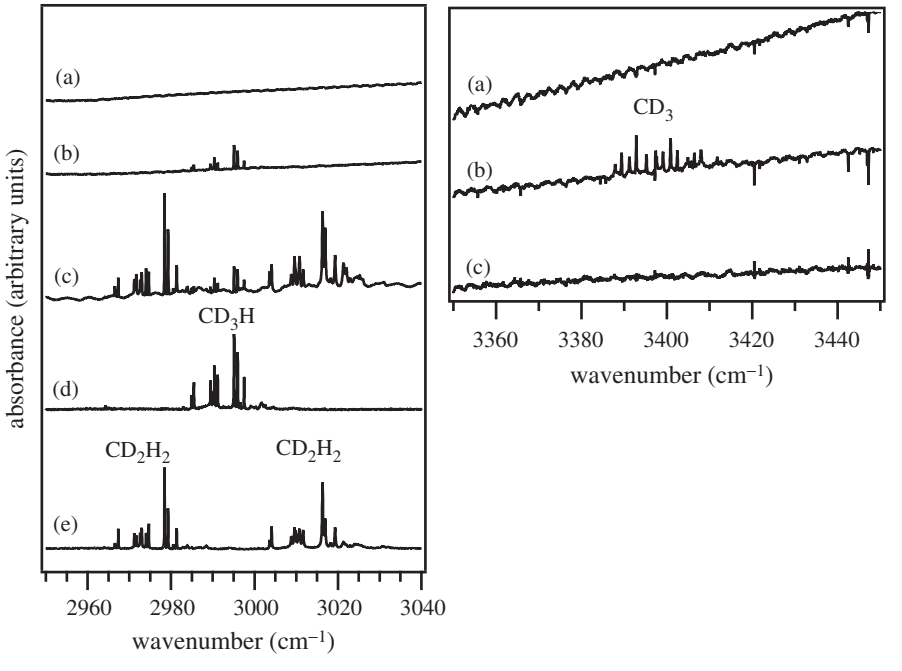

Figure 2. Infrared absorption spectra of CD_3I in solid parahydrogen in the spectral regions 2 950–3 040 cm^{-1} and 3 350–3 450 cm^{-1}. Trace (a): the sample as deposited and recorded before UV irradiation at 253.7 nm. Trace (b): after half-day irradiation with 253.7 nm photons. Trace (c): after subsequent irradiation with 193 nm photons for 20 min. Trace (d): infrared absorption spectrum of isolated CD_3H in solid parahydrogen observed separately. Trace (e): infrared absorption spectrum of isolated CD_2H_2 in solid parahydrogen.

As reviewed in a previous paper [12], the spectral structure of methane in figures 1 and 2 was completely analysed by crystal field theory incorporated with extended group theory [43]. The analysis revealed that rotational motion of methane is slightly hindered in solid parahydrogen. The reduction of the rotational constants is only 10% or less from the gas phase values [13].

The spectral structure of CH_3 and CD_3 radicals seen in trace (c) of figures 1 and 2 are also attributable to the rotational branches subjected to the crystal field fine splitting. The degeneracy of the quantum number M, which is the projection of rotational angular momentum along the crystal axis, is lifted due to the anisotropic electric fields of the parahydrogen lattice. Analysis of the spectral structure revealed that the rotational motion of the methyl radicals is only slightly hindered as in the case of methane; the reduction of the rotational constants is about 10% from the gas phase values [44]. The spectrum of the spin–orbit transition of iodine atoms was also observed at $7638\,cm^{-1}$ [42], which is not shown here. The spectral structure of the spin–orbit transition indicated that some of the produced CH_3 radicals were trapped in a crystal lattice very close to an iodine atom, but the rest of the radicals were completely separated from iodine atoms.

The spectral changes shown in figures 1 and 2 are summarized as follows. The 253.7 nm irradiation of CH_3I in solid parahydrogen yielded methyl radicals (CH_3) and iodine atoms (I). Half-day irradiation with 253.7 nm photons from a 20 W low-pressure mercury lamp with a Toshiba UV-25 cutoff filter led to the photodissociation of most of the iodides into the radicals. The methyl radicals, CH_3, thus produced were completely stable for a few days in solid parahydrogen at 4.5 K. No production of methane was observed at this stage [18, 19]. As for the irradiation of CD_3I by 253.7 nm photons, a small amount of CD_3H was observed in addition to CD_3 radicals. The decrease of the absorption of the CD_3 radicals was observed in a time-scale of a week without irradiation of any radiation, and the increase of the absorption of CD_3H was observed concomitantly (see figure 3). Right after the production of the methyl radicals in solid parahydrogen, the radical was excited by 193 nm UV pulses. Twenty-minute irradiation with UV pulses from an ArF excimer laser (6 mJ/pulse, 30 Hz) was enough to destroy most of the radicals. Along with the destruction of the radicals, the formation of methane CH_4 was observed as seen in figure 1. The 193 nm irradiation of CD_3 in solid parahydrogen yielded CD_2H_2, but did not yield CD_3H as is clearly seen in trace (c) of figure 2.

Reaction schemes consistent with these experiments are as follows.

$$CH_3I + h\nu(253.7\,nm) \rightarrow CH_3^{\dagger} + I \rightarrow CH_3 + I \tag{1}$$

$$CH_3 + h\nu(193\,nm) \rightarrow CH_3^{*}(\tilde{B}^2A_1') \rightarrow CH_2(\tilde{a}^1A_1) + H \tag{2}$$

$$CH_2(\tilde{a}^1A_1) + H_2 \rightarrow CH_4 \tag{3}$$

UV light at 253.7 nm produces methyl radicals with an excess energy ($CH_3^{\dagger}$), but the radical is deactivated to its ground state quickly as in reaction (1). Since methyl radicals absorb at wavelengths shorter than 216 nm, to be excited to a 3*s* Rydberg state ($\tilde{B}^2A_1'$) [45, 46], the deactivated radical reabsorbs light at 193 nm as in

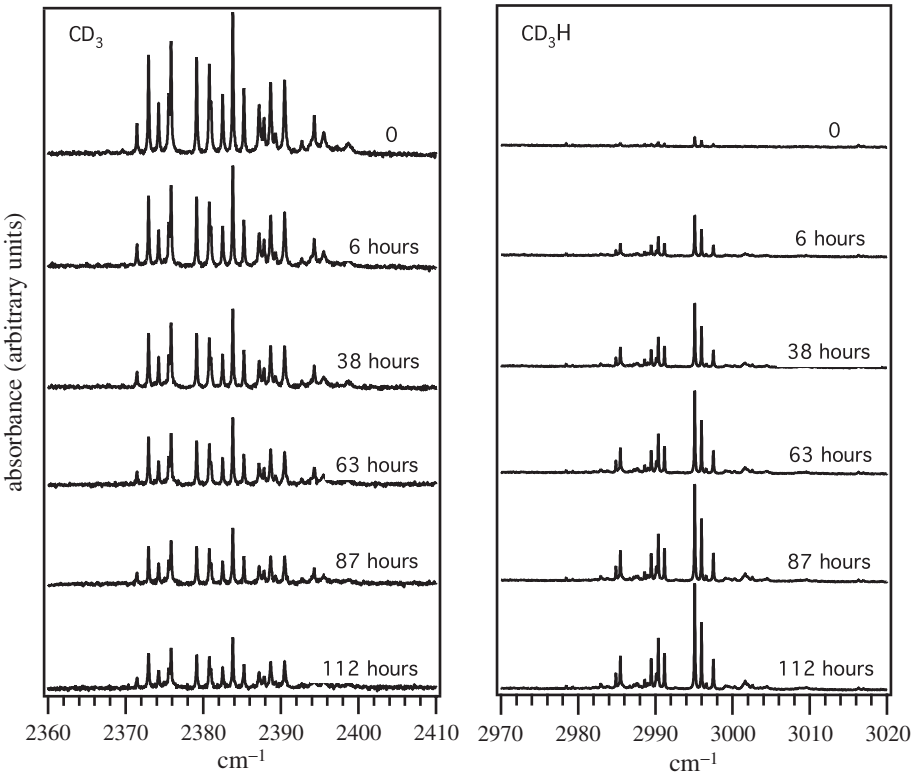

Figure 3. Spectral changes of infrared absorption of CD_3 (left) and CD_3H (right) in solid parahydrogen. The sample was kept at 4.5 K in a completely dark condition except for the recording period of each FTIR spectrum. The CD_3 radical was prepared by the *in situ* photolysis of CD_3I in solid parahydrogen.

reaction (2). The excited radical in the $\tilde{B}$ state dissociates into a singlet methylene ($\tilde{a}^1A_1$) and a hydrogen atom (^2S) [47, 48], the former executing the insertion reaction with a nearby hydrogen molecule to be methane as in reaction (3) [49].

A subpicosecond dynamics study [47] and photofragment translational spectroscopic study [48] in the $\tilde{B}^2A_1'$ state of the methyl radical have disclosed a rapid dissociation into single methylene [CH_2 ($\tilde{a}^1A_1$)] and H. The barrier height of this dissociation in the $\tilde{B}$ state is estimated to be 2200 cm^{-1} [47]. Since the photon energy of 193 nm radiation (51 800 cm^{-1}) is sufficiently larger than the dissociation barrier height of 48 500 cm^{-1} measured from the ground state of methyl radical, there should be ample energetic allowance for the whole sequence of reaction (2). Once singlet methylene is formed, it reacts with a nearby hydrogen molecule directly with no barrier as in reaction (3) [50].

One may conceive that the kinetic methyl radicals $CH_3^\dagger$ in reaction (1) undergo the collision-induced reaction (4) below.

$$CH_3^\dagger + H_2 \rightarrow CH_4 + H \qquad (4)$$

Translational and internal energy partitioning in the methyl and iodine fragments formed from photodissociation of methyl iodide in the A-band region has been extensively studied using time-of-flight (TOF) [51, 52] and velocity mapping measurements [53] as well as using high-resolution infrared diode laser spectroscopy [54]. The $n \rightarrow \sigma^*$ electronic excitation to the lowest lying A-band absorption leads to two dissociation channels, that is, $CH_3 + I^*(^2P_{1/2})$ and $CH_3 + I(^2P_{3/2})$. Methyl radicals produced in conjunction with $I(^2P_{3/2})$ have higher excess energy. Referring to the measurements of kinetic energy distributions of CH_3 radicals at various dissociation wavelengths in the range 240–330 nm [53], the kinetic energy of CH_3 radical fragments in the $v = 0$ vibrational ground state produced in conjunction with $I(^2P_{3/2})$ is estimated to be about 18 000 cm^{-1} by the excitation of 253.7 nm radiation, while that in conjunction with $I^*(^2P_{1/2})$ is about 11 000 cm^{-1}. Since the activation energy of the thermal reaction between a methyl radical and a hydrogen molecule is known to be less than 5000 cm^{-1} [55, 56] which is by far smaller than the kinetic energies of the CH_3 radical fragments, the collision-induced reaction (4) is energetically allowed for the CH_3 radicals produced by both channels. However, the possibility of reaction (4) is completely ruled out as no absorption of CH_4 was observed in trace (b) in figure 1. The failure of the formation of methane at 253.7 nm indicates that the conversion from the translational energy of $CH_3^\dagger$ to the internal energy for the large-amplitude motion to accomplish reaction (4) is inefficient. Instead, the translational energy of $CH_3^\dagger$ is probably rapidly transferred to phonons of solid hydrogen. The presumed rapid dissipation of the excess energy to phonons is probably due to the distinctly high thermal conductivity of solid parahydrogen [39].

The abstraction of a hydrogen atom from a hydrogen molecule by the excited radical in the $\tilde{B}$ state is also conceivable for the production of methane as in reaction (5).

$$CH_3^*(\tilde{B}^2A_1') + H_2 \rightarrow CH_4 + H \tag{5}$$

However, the possibility of reaction (5) can be ruled out by the parallel study of photolysis of CD_3I in solid parahydrogen. In the deuterated system, the production of CD_3H is expected by the deuterated analogue of the abstraction reaction (5), but no appreciable increase of the absorption of CD_3H was observed in trace (c) of figure 2, which indicates that reaction (5) cannot be dominant.

Another possibility for the production of methane is the reaction of methyl radicals in the electronic ground state with nearby hydrogen molecules:

$$CH_3(\tilde{X}^2A_2'') + H_2 \rightarrow CH_4 + H \tag{6}$$

The reaction (6) must proceed via tunnelling [18, 23], which will be discussed in section 6 in detail. In the case of deuterated CD_3, we found that the reaction actually took place in a time-scale of a few days. The small absorption of CD_3H in trace (b) of figure 2 is entirely attributable to methane produced by the tunnelling reaction (6). On the other hand, CH_3 did not react with nearby hydrogen molecules even after a week; see section 6. In any case, the time-scale of reaction (6) is one or more orders of magnitude longer than the time-scale of experiments shown in

figures 1 and 2; it is concluded that the methane molecules observed in trace (c) of figures 1 and 2 were not produced by reaction (6).

A hydrogen atom, H, produced by reaction (3) may migrate in solid parahydrogen to encounter another radical to produce methane.

$$CH_3 + H \rightarrow CH_4 \tag{7}$$

The diffusion rate of a hydrogen atom in our sample was experimentally determined from the photolysis study of NO [22]. The rate at about 5K was such that migrated H atoms encounter an impurity molecule in a time-scale of about 1000 min. in a sample containing 1×10^{21} molecules m^{-3} of impurities. The CH_3 radicals, however, were found to stay in any crystal over a week after UV irradiation, which implies that the reaction (7) cannot be dominant [18, 19]. In fact, most hydrogen atoms recombined with iodine atoms to produce HI as evidenced in the spectral change of the spin–orbit absorption of iodine atoms.

In summary, the photolysis of methyl iodides and methyl radicals took place efficiently in solid parahydrogen, and the reaction schemes are exclusively those shown in reactions (1), (2) and (3).

5. Nuclear spin selection rule in chemical reactions

It has been discussed that nuclear spin angular momentum is conserved in chemical processes, where particle rearrangements occur [57, 58]. The nuclear spin selection rule in chemical reactions plays an important role in various fields, especially in interstellar chemistry [59–64]. Observation of the abundance of each nuclear spin state of a molecule provides a key to understanding the formation of the molecule in interstellar space.

Despite the importance of the selection rule, only a few experimental studies have been reported so far on the quantitative analysis of the nuclear spin modification during chemical reactions [36, 65–71]. Selective generation of *ortho*-H_2 by the photodissociation of *ortho*-H_2CO [68, 69] provides evidence for nuclear spin conservation. Other evidence is the nuclear spin selection rule in an ion–molecule reaction $H_2^+ + H_2 \rightarrow H_3^+ + H$ [70, 71]. Nevertheless, these experiments were performed at relatively high temperature, where the thermal distribution of each rotational level of molecules made the analysis quite complicated.

The consecutive reactions (2) and (3) described in the previous section are an ideal system to examine the nuclear spin selection rule in chemical reactions [36]. The methyl radical, CH_3, has two distinct nuclear spin states of $I = 3/2$ and $I = 1/2$, while methylene, CH_2, and the hydrogen molecule, H_2, have two nuclear spin states of $I = 1$ and $I = 0$, respectively. Methane, CH_4, has three different nuclear spin states, that is, $I = 2(A)$, $I = 1(F)$, and $I = 0(E)$ [72]. Since the reactants CH_3 occupy only the lowest rotational level at 4.5K, one can easily examine the conservation rule from the intensity of high-resolution infrared absorption spectrum of the product (CH_4).

Methane, CH_4, has three different nuclear spin states, and each nuclear spin state couples to particular rotational states. The $J=0$ rotational state of CH_4 couples to the $I=2$ nuclear spin state, the $J=1$ couples to the $I=1$ state, the $J=2$ couples to both the $I=1$ and $I=0$ states, and so on [72]. In other words, the lowest rotational state of each nuclear spin state is the $J=0$ state for the $I=2$ nuclear spin state, the $J=1$ state for the $I=1$ state, and the $J=2$ state for the $I=0$ state. Thus, the population of each nuclear spin state can be determined directly from the intensities of rotationally resolved infrared absorption spectra at low temperature.

In order to determine the population ratio from the intensity of each rotational branch, one must know the absolute transition intensity of each transition. However, there is always some ambiguity in determining the absolute transition intensity especially in condensed phases. In this study, instead of using the information of absolute intensity, we determined the population ratio of each nuclear spin state from the analysis of nuclear spin conversion of methane in solid parahydrogen [36].

As we discussed in separate papers [73–75], conversion among the three nuclear spin states of CH_4 takes place in solid parahydrogen. Relaxation from the $J=2$, $I=0$ state to lower states was extremely fast, so that we never observed absorption from the $J=2$, $I=0$ state. On the other hand, relaxation from the $J=1$, $I=1$ state to the $J=0$, $I=2$ state took place in a time-scale of a day. Temporal changes of the mole fraction $c(t)$ of the $I=2$ nuclear spin state were well fitted with the function

$$c(t) = [c(0) - c(\infty)]\exp(-kt) + c(\infty), \tag{8}$$

where $c(0)$ and $c(\infty)$ are the mole fraction at $t=0$ and $t=\infty$, respectively, and k is the conversion rate, which is a function of temperature. The rate at 4.6 K was found to be $k = 2.8 \times 10^{-3}\,\mathrm{min}^{-1}$ [75].

In the present reaction system, the initial nuclear spin population of CH_4 just after the reaction can be obtained from the value of $c(0)$ in equation (8). Since the population in the $I=0$ nuclear spin state is negligible, the ratio $c(0)/(1-c(0))$ corresponds to the population ratio between the $I=2$ and $I=1$ states. Note that the population in the $I=1$ nuclear spin state we observed should be considered as the sum of the population of the $I=1$ and $I=0$ nuclear spin states after the reaction, since all the $J=2$, $I=0$ state had relaxed to the $J=1$, $I=1$ state within our experimental time-scale [75].

From the analysis of the nuclear spin conversion, the initial mole fraction of the $I=2$ state just after the reactions was obtained to be $c(0)=0.19\pm0.01$ [36]. The uncertainty in the fraction was estimated to be less than 5%. Therefore, it is concluded that the population of each nuclear spin state of CH_4 just after the consecutive reactions (2) and (3) was $[I=2]:([I=1]+[I=0]) = 0.2:0.8$ with an uncertainty of 5%.

The initial population ratio of $[I=2]:([I=1]+[I=0]) = 0.2:0.8$ is significantly different from the equilibrium ratio at the high temperature limit of $[I=2]:[I=1]:[I=0] = 0.31:0.56:0.13$ [76, 77], or $[I=2]:([I=1]+[I=0]) = 0.31:0.69$. Furthermore, it is also significantly different from the equilibrium population ratio at 4.6K of $[I=2]:[I=1]:[I=0] = 0.9:0.1:0.0$. If there is no selection rule on the nuclear spin modification in the chemical reaction, the initial population must be that

of the high temperature limit because of the excess energy in reactions (2) and (3). The significant population in the $I=1$ state after the reaction indicates that the nuclear spin selection rule does exist in the present reaction system.

What population ratio would we expect if nuclear spin is conserved during the processes that led from the CH_3 precursor to the CH_4 product? The nuclear spin selection rule in the photodissociation reaction (2) predicted by the theory is shown in table 1(a) [36]. The $I=1/2$ CH_3 radical produces both the $I=0$ and $I=1$ nuclear spin states of CH_2, while the $I=3/2$ radical results in only the $I=1$ state of CH_2. Table 1(b) lists the nuclear spin selection rule in reaction (3). We assumed that reaction (3) is the insertion reaction as in the gas phase [49].

The nuclear spin of the $N=0$, $K=0$ rotational state of the methyl radical in the ground electronic state is $I=3/2$, while that of the $N=1$, $K=1$ state is $I=1/2$ [72]. The analysis of the infrared absorption of CH_3 in solid parahydrogen revealed that all the radicals were in the $N=0$, $K=0$ lowest rotational state in solid parahydrogen. Although the $N=1$, $K=1$ state is the lowest rotational state for the $I=1/2$ methyl radical, nuclear spin conversion from the $I=1/2$ state to the $I=3/2$ state must be fast enough, so that all the radicals relax into the $N=0$, $K=0$ ground rotational state before the initiation of photolysis at 193 nm.

Since the methyl radical in the present system occupied the $I=3/2$ state only, the nuclear spin state of $^1CH_2$ produced by the UV irradiation is $I=1$ exclusively as shown in table 1(a). Then, the produced $^1CH_2$ undergoes the insertion reaction with a hydrogen molecule H_2. Since more than 99.9% of hydrogen molecules in our sample were parahydrogen ($I=0$), only the $I=1$ CH_4 is produced after the reaction (3) as shown in table 1(b). In summary, the nuclear spin states relevant to the present system are exclusively

$$^2CH_3(I=3/2) \rightarrow {}^1CH_2(I=1) + H \tag{9}$$

and

$$^1CH_2(I=1) + H_2(I=0) \rightarrow CH_4(I=1) \tag{10}$$

Thus, the population of CH_4 after the reaction is expected to be $[I=2]:[I=1]:[I=0]=0.0:1.0:0.0$, if the nuclear spin conservation rule is perfect. The observed

Table 1. (a) Ratio of the nuclear spin isomers of $^1CH_2$ produced by the photolysis of CH_3. (b) Ratio of the nuclear spin isomers of CH_4 after the insertion reaction of $^1CH_2+H_2 \rightarrow CH_4$.

(a) CH_3	$\rightarrow$	$^1CH_2$			+	H
		$[I=0]$	:	$[I=1]$		
$I=1/2$		1	:	1		
$I=3/2$		0	:	1		

(b) $^1CH_2$	+	H_2	$\rightarrow$	CH_4				
				$[I=2]$	:	$[I=1]$	:	$[I=0]$
$I=0$		$I=0$		0	:	0	:	1
$I=1$		$I=0$		0	:	1	:	0
$I=0$		$I=1$		0	:	1	:	0
$I=1$		$I=1$		1	:	1	:	1

80% population in the $I=1$ state after the reaction clearly indicates that the nuclear spin selection rule does exist in the present reaction system.

Note that we have observed about 20% population in the $I=2$ state of CH_4 just after the reaction, which is not predicted by the theory. One possible explanation for the production of the $I=2$ state is that the nuclear spin selection rule is partially violated in the present reaction system. Another explanation is that, although the nuclear spin selection rule holds perfectly, the reaction mechanism in solid parahydrogen is different from that in the gas phase. As for the latter possibility, if the reaction between a methylene and a hydrogen molecule is not the insertion reaction, but a successive abstraction reaction

$$CH_2 + H_2 \rightarrow CH_3 + H \rightarrow CH_4 \tag{11}$$

the production of the $I=2$ nuclear spin state is expected. Table 2 summarizes the nuclear spin selection rule involved in the above stepwise reaction [36]. The $I=2$ CH_4 is produced by the reaction between the $I=3/2$ CH_3 radical and $I=1/2$ H atom. The stepwise reaction of the $I=1$ CH_2 and $I=0$ H_2 results in the nuclear spin population of CH_4 as $[I=2]:[I=1]:[I=0]=0.25:0.5:0.25$, or $[I=2]:([I=1]+[I=0])=0.25:0.75$. Thus, a combination of the insertion reaction (3) and the abstraction reaction (11) might explain the 20% population in the $I=2$ state produced by the UV photolysis of CH_3.

It is known that the reaction between a singlet methylene $^1CH_2$ and a hydrogen molecule H_2 is the insertion reaction, while the reaction between a triplet methylene $^3CH_2$ and a hydrogen molecule H_2 is the abstraction reaction [78, 79]. Thus, if some of the singlet methylenes $^1CH_2$ relax to the triplet state before the reaction with H_2, the $I=2$ CH_4 could be produced by the stepwise reaction in reaction (11). However, the possibility of the reaction path via $^3CH_2$ may be denied, since the relaxation rate from the singlet $^1CH_2$ to the triplet $^3CH_2$ is two orders of magnitude slower than the rate of the insertion reaction [49, 80]. In fact, no infrared absorption corresponding to $^3CH_2$ [81] was observed at any stage of the present experiment.

Table 2. (a) Ratio of the nuclear spin isomers of CH_3 produced by the abstraction reaction of $CH_2+H_2\rightarrow CH_3+H$. (b) Ratio of the nuclear spin isomers of CH_4 after the reaction of $CH_3+H\rightarrow CH_4$.

(a) CH_2	+	H_2	→	CH_3			+	H
				$[I=3/2]$	:	$[I=3/2]$		
$I=0$		$I=0$		0	:	1		
$I=1$		$I=0$		1	:	1		
$I=0$		$I=1$		1	:	1		
$I=1$		$I=1$		1	:	1		

(b) CH_3	+	H	→			CH_4		
				$[I=2]$	:	$[I=1]$	:	$[I=0]$
$I=3/2$		$I=1/2$		1	:	1	:	0
$I=1/2$		$I=1/2$		0	:	1	:	1

Nevertheless, because of the proximity between CH_2 and H_2 in the solid, the stepwise reaction in reaction (11) may proceed even via $^1CH_2$ as a result of the long interaction time between CH_2 and H_2. The wavefunction of H_2 could partially overlap with CH_2 due to the large amplitude of zero-point lattice vibrations, which may induce the abstraction reaction instead of the insertion reaction. The long interaction time between reactants is one of the important features of low-temperature chemistry, which could open different reaction pathways that are supposed to be forbidden at high temperatures.

In any case, the experimental result indicated clearly and definitively that the nuclear spin selection rule does exist, but the rule seems to be partially violated in the present system. Further studies, both theoretically and experimentally, are necessary for more quantitative understanding of the present reaction system, from which we would obtain further information on the nuclear spin selection rule in chemical reactions as well as chemical reactions at low temperatures.

6. Tunnelling chemical reactions

Other important evidence of the reaction relevant to the present system is the reaction of a methyl radical in the ground electronic state with a nearby hydrogen molecule (reaction 6). Since the activation energy of the above reaction is estimated to be 11–14 kcal mol^{-1} ($\simeq$ 5500–7000K) [55, 56], the occurrence of reaction (6) at 4.5 K must be ascribed exclusively to pure tunnelling.

Tunnelling reaction is the reaction through a barrier, which is a pure quantum effect. The existence of tunnelling effects in chemical reactions was first discussed by Wigner [82]. Many theoretical works have been reported since then [83–85], whereas few direct indications of tunnelling effects in chemical reactions have been observed experimentally. Most studies were done at high temperatures, where thermally activated reactions suppress the possible tunnelling pathways. Under normal conditions, the tunnelling effect in chemical reactions is barely obtained.

In the present system, we have obtained direct evidence of the tunnelling reaction of the type $X + H_2 \rightarrow XH + H$. We have studied reactions of all isotopomeric radicals CD_3, CD_2H, CDH_2 and CH_3, and found a clear effect of deuteration on tunnelling rate as described below [18, 23].

Figure 3 shows the temporal behaviour of the absorption of CD_3 and CD_3H in a sample kept at 4.5 K without being irradiated by any photons. A decrease in the absorption intensity of CD_3 and concomitant increase in the intensity of CD_3H were observed over a span of about one week. It is clear that CD_3 reacted with surrounding hydrogen molecules through the tunnelling reaction

$$CD_3 + H_2 \rightarrow CD_3H + H \tag{12}$$

We have observed similar spectral changes in the systems of CD_2H and CDH_2. On the other hand, no appreciable changes in the intensity of CH_3 and CH_4 were observed under the same conditions. Figure 4 shows the plot of intensity of CH_3 in a sample

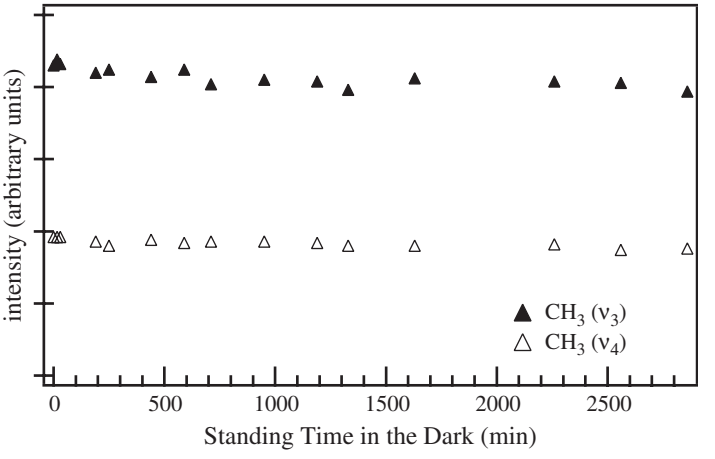

Figure 4. Temporal behaviour of the intensity of the ν_3 and ν_4 absorption of CH_3 in solid parahydrogen. The sample was kept at 4.5K in a completely dark condition except for the recording period of each FTIR spectrum.

kept at 4.5 K. No appreciable changes in the intensity of CH_3 were observed over a few days, indicating that the tunnelling reaction between the CH_3 radical and parahydrogen does not occur or is too slow to detect in our experimental time-scale.

$$CH_3 + H_2 \not\rightarrow CH_4 + H \tag{13}$$

The temporal changes of the intensity of CD_3 and CD_3H shown in figure 3 were found to be well described by the following equations,

$$I_{CD_3}(t) = Ce^{-kt} \tag{14}$$

$$I_{CD_3H}(t) = C'(1 - C''e^{-kt}) \tag{15}$$

except for the minor contribution of other reactions initiated by the presence of an iodine atom [23]. Here, k is the first-order reaction rate, and C, C', and C'' are arbitrary constants. Although the reaction (12) is a bimolecular reaction, the reaction in the present system should be treated as a unimolecular reaction, because the reaction rate in the present system does not depend on the concentration of H_2; all the radicals were surrounded by 12 H_2 molecules with an equal distance of $\sim$3.8 Å at all times. The first-order rate constants k determined by the least-squares fitting of the above equations for each deuterated system are listed in table 3(a). Note that the rate listed for CH_3 in table 3 is the upper limit of the tunnelling rate.

The crux of the present work is the finding that the reaction of CD_3 took place while the reaction of CH_3 did not under the same experimental conditions. Furthermore, the tunnelling rate increases as the degree of deuteration of the radicals increase.

Table 3. First-order rate constants of the tunnelling reaction of $X + H_2 \rightarrow XH + H$ ($X = CD_3$, CD_2H, CDH_2 and CH_3). The numbers in the table represent the first-order rate constant (k) in units of s^{-1}.

		CD_3	CD_2H	CDH_2	CH_3
(a)	without filters	3.2×10^{-6}	1.3×10^{-6}	1.0×10^{-6}	$<1 \times 10^{-8}$ (c)
(b)	with a filter				
	2 170–3 905 cm^{-1}	3.5×10^{-6}	2.0×10^{-6}	–	–
	1 330–2 240 cm^{-1}	–	–	1.0×10^{-6}	–
	785–1 390 cm^{-1}	3.5×10^{-6}	–	–	–

(a) No filters were used during the recording of FTIR spectra. The sample was exposed to a weak IR source of 700–7 500 cm^{-1} during the recording.
(b) A filter transmitting the range specified in the first column was placed between the globar source and the sample. There are several absorptions corresponding to the stretching and bending motion of both methyl radicals and methane molecules in the regions of 2 170–3 905 cm^{-1} and 1 330–2 240 cm^{-1}. There is only one absorption corresponding to the bending motion of CD_3H molecules, but no absorption of CD_3 in the region of 785–1 390 cm^{-1}.
(c) Upper limit of the rate constant.

The clear cut-off difference between CH_3 and other deuterated systems may be ascribed to the difference in the enthalpy including the zero-point energies of the reactants and products [18, 23]. The reaction between the methyl radical and hydrogen molecule is nearly thermoneutral since the zero-point dissociation energies of H_2 ($D_0 = 4.4781$ eV) [86] and CH_4 ($D_0 = 4.406$ eV) [45] are very close. Consequently, the small difference in zero-point vibrational energies would cause a drastic change in the occurrence of the tunnelling reactions. The differences of zero-point energies between the reactants and products are estimated to be 881 cm^{-1}, 949 cm^{-1}, 1005 cm^{-1}, and 1060 cm^{-1} for the CD_3, CD_2H, CDH_2, and CH_3 system, respectively, where a positive value means that the zero-point vibrational energy of products is larger than that of reactants. The difference of the total electronic energies of the reactants and products without the zero-point energy correction is so close that it is not yet certain. Assuming that the total electronic energy of the reactants without zero-point correction is, for example, 1050 cm^{-1} higher than that of the products, the reactions of CD_3, CD_2H, and CDH_2 are all endothermic, while the reaction of CH_3 is exothermic by 10 cm^{-1} due to the zero-point energy correction. When the total energy of the products including the zero-point energy is higher than that of the reactants, no reaction between the radical and H_2 is expected. Since the reactants and products in the present system are not freely moving as in the gas phase, but are trapped in cages formed by the parahydrogen matrix, the actual endothermicity could be slightly different from that in the gas phase. For example, the H atom that is produced in the reaction may contribute an additional zero-point contribution to the product side of the reaction. In any case, the difference in zero-point vibrational energies could be the origin of the clear-cut difference between CH_3 and other systems.

The difference in the potential energy surface of the whole reaction path may also explain the increase of the tunnelling rate by increasing the degree of deuteration. The potential energy surface of the whole reaction path is slightly different for different degrees of deuteration due to the difference in zero-point vibrations. Tunnelling rate must be sensitive to such small differences in the potential energy surfaces. Recent theoretical calculations predicted the difference in reaction rates between CH_3 and

CD_3 by one order of magnitude [56]. However, the difference in the tunnelling rate between CH_3 and CD_3 is still smaller than that determined experimentally (more than two orders of magnitude). More precise theoretical study is indispensable in order to understand the clear dependence on the degree of deuteration.

Note that the nuclear spin selection rule described in the previous section could play a role in the clear-cut difference between CH_3 and other deuterated systems. If the tunnelling reaction takes place via a CH_5 intermediate molecule, the nuclear spin selection rule relevant to the present system becomes

$$CH_3(I = 3/2) + H_2(I = 0) \rightarrow CH_5(I = 3/2) \rightarrow CH_4(I = 1) + H \tag{16}$$

Therefore, the lowest $J = 0$, $I = 2$ state is not accessible due to the selection rule, while the $J = 1$, $I = 1$ CH_4 is accessible whose energy is about $8.8\,cm^{-1}$ higher than the lowest state [13]. The difference of $8.8\,cm^{-1}$ is small compared with the difference in zero-point energies, but the selection rule actually makes the tunnelling reaction (16) slightly unfavourable. On the other hand, if the reaction is a one-step abstraction reaction as in reaction (6), all the nuclear spin isomers of methane are expected to be produced directly, and therefore the nuclear spin selection rule does not play any role in the effect of deuteration.

Another possible selection rule is that imposed by the quantum statistics, as the present reactants and products consist of different numbers of fermions (H) and bosons (D) [87]. However, it is too early to discuss this kind of selection rule in the chemical reaction of polyatomic molecules at the moment.

One thing we would like to point out is that the weak probe IR light was found to affect the tunnelling rates slightly. The effect of probe light on the tunnelling rate is summarized in table 3(b). A disadvantage of using an FTIR spectrometer for the observation of the tunnelling reaction is that the sample is exposed to the light source of the spectrometer during scans. Since the tunnelling rate must depend on the quantum number of the vibration–rotation states of reactants, excitation by the light source, although very weak, may change the overall reaction rate. Fortunately, as shown in table 3, the effect of the light source on the rate of the CD_3 and CDH_2 systems was found to be negligibly small. On the other hand, a slight increase in the tunnelling rate of CD_2H was observed when the IR beam was filtered out except for the region of $2170–3905\,cm^{-1}$ as shown in table 3. The tunnelling effect is so sensitive that negligibly small changes of environment induced by the weak probe IR light may affect the tunnelling rate. However, it remains totally unexplained at the moment. The problem awaits further studies.

Quantum tunnelling in chemical reactions has long attracted chemists' interest [83–85]. The nonlinearity of the Arrhenius plot of reaction rate constant versus the inverse of temperature is taken customarily as an indication of the involvement of tunnelling. However, the nonlinearity itself should not necessarily be attributed to tunnelling because of other possible causes such as the temperature dependent effect of the environment. Therefore, convincing evidence for tunnelling based on the temperature dependence of reaction rate constants is scarce [88]. Studies of chemical reactions in solid parahydrogen will contribute to answering this long-standing question.

7. Conclusion

This article surveys our recent work on photolysis of methyl iodide and subsequent reactions in solid parahydrogen. There remain many unsolved problems even in such a simple reaction system as described in this article. Low-temperature chemistry is becoming important in connection with molecular evolution in interstellar space [89] as well as recent developments in making cold molecules [90, 91]. Studies of chemical reactions in solid parahydrogen, or quantum crystals, is undoubtedly a potential method for the understanding of nature of low-temperature chemistry.

Acknowledgement

This study was partially supported by Grant-in-aid for Scientific Research of the Ministry of Education, Science, Culture, and Sports of Japan.

References

[1] G. N. Lewis, D. Lipkin, and T. T. Magel, J. Am. Chem. Soc. **63,** 3005 (1941).
[2] M. E. Jacox, J. Phys. Chem. Ref. Data, **27,** 115 (1998).
[3] V. E. Bondybey and V. A. Apkarian, Chem. Phys. **189,** 137 (1994).
[4] I. Norman and G. Porter, Nature **174,** 508 (1954).
[5] I. L. Mador, J. Chem. Phys. **22,** 1617 (1954).
[6] G. C. Pimentel, in *Formation and Trapping of Free Radicals*, edited by A. M. Bass and H. P. Broida (Academic, New York, 1960), p. 69.
[7] L. Andrews and G. C. Pimentel, J. Chem. Phys. **47,** 3637 (1967).
[8] L. E. Brus and V. E. Bondybey, J. Chem. Phys. **65,** 71 (1976).
[9] T. Momose, M. Miki, M. Uchida, T. Shimizu, I. Yoshizawa, and T. Shida, J. Chem. Phys. **103,** 1400 (1995).
[10] S. Tam, M. Macler, and M. E. Fajardo, J. Chem. Phys. **106,** 8955 (1997).
[11] T. Momose, and T. Shida, Bull. Chem. Soc. Jpn. **71,** 1 (1998).
[12] T. Momose, H. Hoshina, M. Fushitani, and H. Katsuki, Vib. Spectrosc. **34,** 95 (2004).
[13] T. Momose, M. Miki, T. Wakabayashi, T. Shida, M. C. Chan, S. S. Lee, and T. Oka, J. Chem. Phys. **107,** 7707 (1997).
[14] S. Tam, M. E. Fajardo, H. Katsuki, H. Hoshina, T. Wakabayashi, and T. Momose, J. Chem. Phys. **111,** 4191 (1999).
[15] H. Hoshina, T. Wakabayashi, T. Momose, and T. Shida, J. Chem. Phys. **110,** 5728 (1999).
[16] T. Oka, Annu. Rev. Phys. Chem. **44,** 299 (1993).
[17] C. M. Lindsay, T. Oka, and T. Momose J. Mol. Spectrosc. **218,** 133 (2003).
[18] T. Momose, H. Hoshina, N. Sogoshi, H. Katsuki, T. Wakabayashi, and T. Shida, J. Chem. Phys. **108,** 7334 (1998).
[19] M. Fushitani, N. Sogoshi, T. Wakabayashi, T. Momose, and T. Shida, J. Chem. Phys. **109,** 6346 (1998).
[20] M. Fushitani, T. Shida, T. Momose, and M. Rasanen J. Phys. Chem. A **104,** 3635 (2000).
[21] N. Sogoshi, T. Wakabayashi, T. Momose and T. Shida, J. Phys. Chem. A **105,** 3077 (2001).
[22] M. Fushitani and T. Momose, Low Temp. Phys. **29,** 740 (2003).
[23] H. Hoshina, M. Fushitani, T. Momose and T. Shida, J. Chem. Phys. **120,** 3706 (2004).
[24] M. E. Fajardo and S. Tam, J. Chem. Phys. **108,** 4237 (1998).
[25] S. Tam and M. E. Fajardo, Rev. Sci. Instrum. **70,** 1926 (1999).
[26] N. Sogoshi, Y. Kato, T. Wakabayashi, T. Momose, S. Tam, M. E. DeRose, and M. E. Fajardo, J. Phys. Chem. A **104,** 3733 (2000).
[27] M. E. Fajardo and S. Tam, J. Chem. Phys. **115,** 6807 (2001).
[28] S. Tam and M. E. Fajardo, Appl. Spectrosc. **55,** 1634 (2001).
[29] D. T. Anderson, R. J. Hinde, S. Tam, and M. E. Fajardo, J. Chem. Phys. **116,** 594 (2002).
[30] R. J. Hinde, D. T. Anderson, S. Tam, and M. E. Fajardo, Chem. Phys. Lett. **356,** 355 (2002).

[31] K. Yoshioka and D. T. Anderson, J. Chem. Phys. **119,** 4731 (2003).
[32] X. Wang, L. Andrews, S. Tam, M. E. DeRose, and M. E. Fajardo, J. Am. Chem. Soc. **125,** 9218 (2003).
[33] M. E. Fajardo, S. Tam, and M. E. DeRose, and J. Mol. Struct. **695–696,** 111 (2004).
[34] Y.-J. Wu, X. Yang, and Y.-P. Lee, J. Chem. Phys. **120,** 1168 (2004).
[35] H. Hoshina, Y. Kato, Y. Morisawa, T. Wakabayashi, and T. Momose, Chem. Phys. **300,** 69 (2004).
[36] M. Fushitani and T. Momose, J. Chem. Phys. **116,** 10739 (2002).
[37] J. van Kranendonk, *Solid Hydrogen, Theory of the Properties of Solid H_2, HD, and D_2* (Plenum Press, New York, 1983).
[38] L. H. Nosanow, Phys. Rev. **146,** 120 (1966).
[39] I. F. Silvera, Rev. Mod. Phys. **52,** 393 (1980).
[40] D. N. Batchelder, in *Rare Gas Solids*, edited by M. L. Klein and J. A. Venables (Academic, London, 1977), Vol. II, p. 883.
[41] P. C. Souers, *Hydrogen Properties for Fusion Energy* (University of California Press, Berkeley, 1986).
[42] M. Fushitani, T. Momose, and T. Shida, Chem. Phys. Lett. **356,** 375 (2002).
[43] T. Momose, J. Chem. Phys. **107,** 7695 (1997).
[44] H. Hoshina, M. Fushitani, and T. Momose, to be submitted.
[45] G. Herzberg, *Molecular Spectra and Molecular Structure, III, Electronic Spectra and Electronic Structure of Polyatomic Molecules* (Van Nostrand, Princeton, 1966).
[46] H. R. Wendt and H. E. Hunziker, J. Chem. Phys. **81,** 717 (1984).
[47] S. G. Westre, P. B. Kelly, Y. P. Zhang, and L. D. Ziegler, J. Chem. Phys. **94,** 270 (1991).
[48] S. W. North, D. A. Blank, P. M. Chu, and Y. T. Lee, J. Chem. Phys. **102,** 792 (1995).
[49] W. Braun, A. M. Bass, and M. Pilling, J. Chem. Phys. **52,** 5131 (1970).
[50] C. W. Bauschlicher Jr, K. Haber, H. F. Schaefer III, and C. F. Bender, J. Am. Chem. Soc. **99,** 3610 (1977).
[51] S. J. Riley and K. R. Wilson, Chem. Soc. **53,** 132 (1972).
[52] R. Ogorzalek Loo, G. E. Hall, H.-P. Haerri, and P. L. Houston, J. Phys. Chem. **92,** 5 (1988).
[53] A. T. J. B. Eppink and D. H. Parkera, J. Chem. Phys. **110,** 832 (1999).
[54] T. Suzuki, H. Kanamori, and E. Hirota, J. Chem. Phys. **94,** 6607 (1991).
[55] E. Kraka, J. Gauss, and D. Cremer, J. Chem. Phys. **99,** 5306 (1993).
[56] Y. Kurosaki and T. Takayanagi, J. Chem. Phys. **110,** 10830 (1999).
[57] M. Quack, Mol. Phys. **34,** 477 (1977).
[58] T. Oka, J. Mol. Spectrosc. **228,** 635 (2004).
[59] S. Takakuwa, K. Kawaguchi, H. Mikami, and M. Saito, Publ. Astron. Soc. Jpn. **53,** 251 (2001).
[60] Y. C. Minh, W. M. Irvine, and M. K. Brewer, Astron. Astrophys. **244,** 181 (1991).
[61] Y. C. Minh, J. E. Dickens, W. M. Irvine, and D. McGonagle, Astron. Astrophys. **298,** 213 (1995).
[62] J. E. Dickens and W. M. Irvine, Astrophys. J. **518,** 733 (1999).
[63] T. Umemoto, H. Mikami, S. Yamamoto, and N. Hirano, Astrophys. J. **525,** L105 (1999).
[64] Y. Morisawa, M. Fushitani, Y. Kato, H. Hoshina, Z. Simizu, S. Watanabe, Y. Miyamoto, Y. Kasai, K. Kawaguchi, and T. Momose, Astrophys J., in press.
[65] C. R. Bowers and D. P. Weitekamp, Phys. Rev. Lett. **57,** 2645 (1986).
[66] C. R. Bowers and D. P. Weitekamp, J. Am. Chem. Soc. **109,** 5541 (1987).
[67] T. C. Eisenschmid, R. U. Kirss, P. P. Deutsch, S. I. Hommeltoft, R. Eisenberg, J. Bargon, R. G. Lawler, and A. L. Balch, J. Am. Chem. Soc. **109,** 8089 (1987).
[68] B. Schramm, D. J. Bamford, and C. B. Moore, Chem. Phys. Lett. **98,** 305 (1983).
[69] G. Peters and B. Schramm, Chem. Phys. Lett. **302,** 181 (1999).
[70] D. Uy, M. Cordonnier, and T. Oka, Phys. Rev. Lett. **78,** 3844 (1997).
[71] M. Cordonnier, D. Uy, R. M. Dickson, K. E. Kerr, Y. Zhang, and T. Oka, J. Chem. Phys. **113,** 3181 (2000).
[72] E. B. Wilson Jr, J. Chem. Phys. **3,** 276 (1935).
[73] M. Miki and T. Momose, Low Temp. Phys. **26,** 661 (2000).
[74] M. Fushitani and T. Momose, to be submitted.
[75] Y. Miyamoto, M. Fushitani and T. Momose, to be submitted.
[76] A. Amrein, M. Quack, and U. Schmitt, J. Phys. Chem. **92,** 5455 (1988).
[77] M. Hepp, G. Winnewisser, and K. M. T. Yamada, J. Mol. Spectrosc. **164,** 311 (1994).
[78] C. P. Baskin, C. F. Bender, C. W. Bauschlicher Jr, and H. F. Schaefer III, J. Am. Chem. Soc. **96,** 2709 (1974).
[79] L. P. Tan, Chem. Phys. Lett. **57,** 239 (1978).
[80] M. N. R. Ashfold, M. A. Fullstone, G. Hancock, and G. W. Ketley, Chem. Phys. **55,** 245 (1981).
[81] M. D. Marshall and A. R. W. McKellar, J. Chem. Phys. **85,** 3716 (1986).
[82] E. P. Wigner, Z. Phys. Chem. B **19,** 203 (1932).
[83] R. P. Bell, *The Tunneling Effect in Chemistry* (Chapman and Hall, London, 1980).

[84] J. Jortner and B. Pullman, *Tunneling* (Reidel, Dordrecht, 1986).
[85] V. I. Gol'danskii, L. I. Trakhtenberg, and V. N. Fleurov, *Tunneling Phenomena in Chemical Physics* (Gordon and Breach Science, New York, 1989).
[86] K. P. Huber and G. Herzberg, *Molecular Spectra and Molecular Structure IV, Constants of Diatomic Molecules* (Van Nostrand, New York, 1979).
[87] D. J. Heinzen, R. Wynar, P. D. Drummond, and K. V. Kheruntsyan, Phys. Rev. Lett. **84,** 5029 (2000).
[88] W. Siebrand, T. A. Wildman, and M. Z. Zgierski, J. Am. Chem. Soc. **106,** 4083 (1984).
[89] E. Herbst, Ann. Rev. Phys. Chem. **46,** 27 (1995).
[90] H. L. Bethlem and G. Meijer, Int. Rev. Phys. Chem. **22,** 73 (2003).
[91] W. C. Stwalley, Can. J. Chem. **82,** 709 (2004).